# Search for Technicolor Signals with the ATLAS Detector

G. Azuelos, P. Depommier, R. Mazini, and K. Strahl,
Université de Montréal

November 5, 1999

**Abstract:** The discovery potential of multiscale technicolor resonances in ATLAS is studied in a low luminosity scenario. In particular, strategies for a search for the $\rho_T$, $\pi_T$, and $\omega_T$ in various decay channels, and for $b\bar{b}$ and $t\bar{t}$ resonances in $\pi_T$ decays are examined.

Both the Standard Model and supersymmetry predict the existence of a relatively low mass Higgs particle. However, no direct experimental evidence exists, yet, that electroweak symmetry breaking results from the Higgs mechanism operating in the presence of a scalar field. In the Standard Model, requirements of vacuum stability and validity of the running of the effective coupling, in next-to-leading order, limits the allowed range for the mass of the Higgs boson [1]. The theory suffers from problems of triviality and naturalness/hierarchy [2]. Supersymmetry is an appealing alternative since it solves some of these problems, but at the cost of more particles and Higgses, including a light scalar not yet discovered. If no fundamental scalar particle exists, ATLAS will need to be ready for new physics which will need to account for the breaking of electroweak symmetry, for the regularization of the quadri-vector boson coupling, and for providing a mechanism for the generation of mass to the fermions. Understanding the mechanism of electroweak symmetry breaking will require a study, in the high energy regime, of the rate of longitudinal gauge boson pair production, since it's the longitudinal component which provides the mass to these bosons. It will also be essential to search for the presence of new resonances which could regularize the vector boson scattering cross section. This will be one of the primary challenges of ATLAS.

Technicolor theory (TC) provides a dynamical means of breaking the symmetry [3]. It assumes the existence of technifermions possessing a technicolor charge. Classical TC is essentially a replica of QCD with the pion decay constant replaced by the EW scale: 246 GeV. The chiral symmetry of QCD is broken by techniquark condensates giving rise to Goldstone bosons, the technipions, which are the longitudinal degrees of freedom of the W and Z gauge bosons. This simple model is largely ruled out [4] by the present electroweak precision data (S, T and U parameters). The theory has been extended (*extended technicolor*, or ETC) to allow the generation of mass to the known fermions [5], and, in order to account for the absence of FCNC's, the coupling constant is required to "walk", rather than "run". In order to achieve a walking $\alpha_{TC}$, multiscale technicolor models contain several representations of the fundamental family, and lead to the existence of technihadron resonances accessible at LHC energies. Such models, and others [6], are not necesarily excluded by precision electroweak measurements[7, 8]. However, the constraints from these measurements make it unnatural to explain the top quark mass. In top-color-assisted technicolor (TC2) models, the top quark mass arises in large part from a new strong top-color interaction, which is a separate broken gauge sector.

The search for technipions and associated ETC gauge bosons is discussed in recent references [9, 10]. In this note, we shall examine how these predicted resonances can be observed with the ATLAS detector. In particular, we discuss the search for a (I=1, J=1) techni-rho resonance decaying to a pair of gauge bosons, or to a techni-pion and a gauge boson. Single production of a technipion may be detected under particular conditions if it decays to heavy quarks. A clean signal of the techni-omega can also be obtained from the process $pp \rightarrow \omega_T \rightarrow \gamma\pi_T^0$. Although we use as reference certain models, with a given set of parameters, the signals studied here can be considered are generic of any model which predicts resonances. Therefore, we shall present results in each case not only relative to the reference model, but also as lower limits on the $\sigma \times BR$ (cross section times branching ratio) required for observation of the resonance at the $5\sigma$ level.

All the signals and backgrounds discussed in this note have been generated with PYTHIA 6.1 [11]. The trigger acceptance as well as the detector acceptance and resolution effects were simulated with the parametrized Monte Carlo program ATLFAST 1.53 [12], with default values of the parameters. In particular, jets were reconstructed with the cone algorithm, requiring a cone radius of 0.4 and a minimum $E_T$ of 15 GeV. Low luminosity conditions ($\mathcal{L} = 10^{33}$ cm$^{-2}$ s$^{-1}$) are assumed for the energy resolution of jets. Leptons were required to be isolated, meaning that their electromagnetic cluster in the calorimeter were separated from other clusters by $\Delta R > 0.4$ and $E_T < 10$ GeV in a cone $\Delta R = 0.2$ around the lepton. Jets were identified as b-jets if a b-quark of $p_T > 5$ GeV was within a cone radius of 0.2 of the direction of the jet. For b-tagging efficiencies and rejection factors, case 3, in ATLFAST-B was used: i.e. 53% global efficiency and 91% global rejection of non-b jets are assumed.

To study the multiscale technicolor signals, we take as guiding model the theoretical formulation of K. Lane [13, 14], containing two isotriplets of technipions which mix with $W_L$, $Z_L$, with the parameters suggested there: the dimension of the fundamental representation SU(N$_{TC}$) of the technicolor gauge group N$_{TC}$ = 4; the mixing angle between the longitudinal gauge bosons and the technipions, $|\Pi_T >= \sin\chi|W_L > + \cos\chi|\pi_T >$, with $\sin(\chi) = 1/3$; the decay constant of the mixed state $F_T = F_\pi \sin(\chi) = 82$GeV, and a charge of the up-type technifermion $Q_U = 1.0$, $Q_D = 0$. This model has recently been incorporated in PYTHIA6.1 [11]. It should be noted that the decay widths of the $\rho_T$ and the $\omega_T$ depend upon the value of $(Q_U^2 + Q_D^2)$ and upon the masses of these resonances. The branching ratios assumed in the present analysis do not account for possible decays to transversely polarized gauge bosons, as recently calculated in [15].

The Feynman diagrams for the processes examined in this section are shown in fig. 1. The processes proceed by $qq$ fusion. Another note [16] evaluates the importance of the $WW$ process. The decay channels of a techni-rho ($\rho_T$) depend on the assumed masses of the techniparticles. Fig. 2 shows the dominant channels in a space of $m_{\rho_T}$ vs $m_{\pi_T}$. Different "typical" mass scenarios (shown by asterisks in the figure) have been considered here (see table 1).

The first case is chosen because it has been studied for the Tevatron[14]. Other cases are representative of what one may expect to probe at the LHC. When the $\rho_T$ has been chosen to be lighter than $2m_{\pi_T}$ the decay channel $\rho_T \to 2\pi_T$ is kinematically forbidden. It is also be assumed in this present analysis that the $\pi_T$ coupling (and therefore its decay) to the top quark is very small, as may be expected in TC2 theories. This is an approximation, but is certainly true if the mass is lower than $m_t$. A more general case will be considered in the analysis of a $t\bar{t}$ resonance.

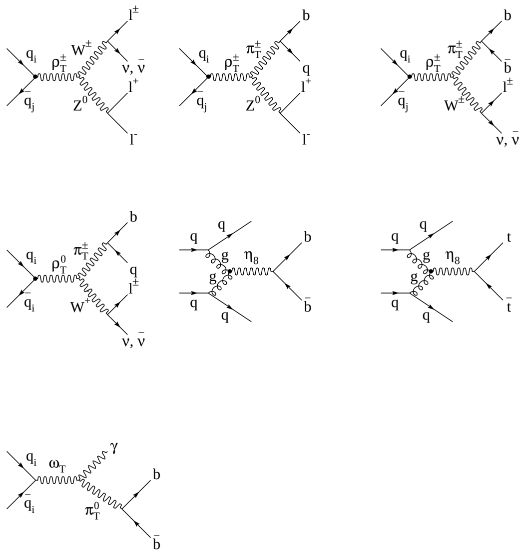

Figure 1: Feynman diagrams for technicolor signals from processes of $q\bar{q}$ and $gg$ fusion

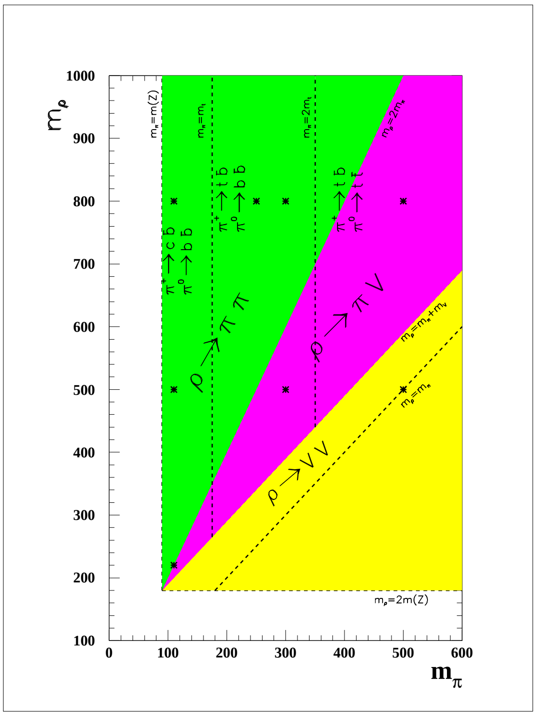


Figure 2: Principal decay channels of the $\rho_T$ and $\pi_T$ in different regions of $m_{\rho_T}$ and $m_{\pi_T}$. The asterisks (*) show the cases studied here

| case | $m_{\rho_T}$ | $\Gamma_{\rho_T^\pm}$ | $\Gamma_{\rho_T^0}$ | $m_{\pi_T}$ | $\Gamma_{\pi_T^\pm}$ | $\Gamma_{\pi_T^0}$ |
|---|---|---|---|---|---|---|
| (a) | 220 | 0.9 | 1.2 | 110 | 0.07 | 0.17 |
| (b) | 500 | 4.5 | 4.6 | 300 | 0.18 | 0.46 |
| (c) | 800 | 7.6 | 7.6 | 500 | 0.30 | 0.77 |
| (d) | 800 | 76.7 | 76.8 | 250 | 0.15 | 0.38 |
| (e) | 500 | 67.0 | 67.2 | 110 | 0.07 | 0.17 |
| (f) | 500 | 1.1 | 1.03 | 500 | 0.30 | 0.76 |
| (g) | 800 | 130.2 | 130 | 110 | 0.07 | 0.17 |
| (h) | 800 | 52.4 | 52.5 | 300 | 0.18 | 0.46 |

Table 1: List of different cases considered in the present analysis. (in GeV)

# 1 $\rho_T^\pm \rightarrow W^\pm Z^0 \rightarrow \ell^\pm \nu \ell^+ \ell^-$

This decay could be the cleanest channel for the detection of a technirho. The good efficiency of the ATLAS detector for lepton detection and missing transverse energy measurement allows clear identification of the W and Z bosons. The resonant production of high mass $WZ$ with W decaying to two jets has been investigated in the framework of the Chiral Lagrangian Model by [17]. Table 2 shows the parameters assumed here for the techniparticles and the number of events used for the signal simulation. Different $\rho_T^\pm$ masses are considered depending on the kinematical region allowed by its decay (Figure 2). The branching ratios quoted account for a preselection on the mass of the hardscattering subsystem ($\hat{m} > 150$, 300, 600 GeV/c$^2$ for $m_{\rho_T^\pm} =$ 220, 500 and 800 GeV/c$^2$ respectively). This preselection was made to limit the number of generated events.

| $m_{\rho_T}$ GeV/c$^2$ | $m_{\pi_T}$ GeV/c$^2$ | $\Gamma_{\rho_T}$ GeV/c$^2$ | BR ($\rho_T \rightarrow WZ$) | $\sigma \times BR$ (pb) | Nb. of events simulated | Nomalization factor |
|---|---|---|---|---|---|---|
| 220 | 110 (a) | 0.93 | 0.13 | 0.16 | $10^4$ | 0.48 |
| 500 | 110 (e) | 67.1 | 0.014 | $1.04 \times 10^{-3}$ | $10^4$ | $3.1 \times 10^{-3}$ |
| | 300 (b) | 4.47 | 0.21 | $1.3 \times 10^{-2}$ | $10^4$ | 0.04 |
| | 500 (f) | 1.07 | 0.87 | $5.4 \times 10^{-2}$ | $10^4$ | 0.16 |
| 800 | 110 (g) | 130.2 | 0.013 | $1.5 \times 10^{-4}$ | $10^4$ | $4.4 \times 10^{-4}$ |
| | 300 (h) | 52.4 | 0.032 | $3.6 \times 10^{-4}$ | $10^4$ | $1.1 \times 10^{-3}$ |
| | 500 (c) | 7.6 | 0.22 | $2.5 \times 10^{-3}$ | $10^4$ | $7.5 \times 10^{-3}$ |

Table 2: Signal parameters for the $\rho_T^\pm \rightarrow W^\pm Z^0 \rightarrow l^\pm \nu l^+ l^-$. Normalization is for 30 fb$^{-1}$

The only background which needs to be considered is the continuum production of WZ gauge bosons, with a cross section of 21 pb. The number of events simulated was

$4 \times 10^4$, with only the leptonic decays $W^\pm \rightarrow l^\pm\nu(\overline{\nu})$, and $Z^0 \rightarrow l^+l^-$ with $l = e, \mu$ (BR = 0.216 and 0.067 respectively).

The applied cuts were the following:

- The lepton trigger serves as a preselection. At least 3 charged leptons ($E_T^\ell > 20$ GeV for $e$'s and 6 GeV for $\mu$'s), two of which must have the same flavour and opposite charge, are required
- the invariant mass of the lepton pair with the same flavour and opposite sign should be close to the that of the $Z$: $m_{l^+l^-} = m_Z \pm 5$ GeV/c$^2$.
- The longitudinal momentum of the neutrino is calculated, within a 2-fold ambiguity, from the missing transverse energy and the momentum of the unpaired lepton assuming an invariant mass $m_{\ell\nu} = m_W$. Both solutions are given a weight of 0.5. Once the $W$ and $Z$ are reconstructed, their transverse momentum is required to be larger than 40 GeV/c (figure 3).
- Only events for which the decay angle with respect to the direction of the WZ system ($\rho_T$) in its rest frame is $|\cos\hat{\theta}| < 0.8$ are accepted.. This variable is sensitive to the polarization of the $\rho_T$ (see fig. 4).

Table 3 shows the number of signal and background events that result from these cuts, for an integrated luminosity of 30 fb$^{-1}$, for all the cases considered. The events were counted in mass regions around the $\rho_T$ peak: [210-240 GeV]. [460-560 GeV] and [740-870 GeV ] for $m_{\rho_T}$=220, 500 and 800 GeV/c$^2$ respectively. No evident signal is observed for cases (e), (g) and (h) (see table 3 and figure 5), principally because the $\rho_T$ resonance is predicted to be wide in these cases. Table 3 shows also the lower limit on $(\sigma \times BR)$ required for a $5\sigma$ significance, from which one could infer the potential of observabilty for a different assumed branching ratio. Since this signal is based only on lepton reconstruction, the significance can be expected to scale approximately as the square root of the integrated luminosity, even in the presence of pile-up.

## 2 $\rho_T^\pm \rightarrow \pi_T^\pm Z^0 \rightarrow bq\ell^+\ell^-$

Here, the technipion decays to b and c quarks (a c-quark jet will not be distigiushed from a light quark jet in this analysis). Only cases (b), (c) and (d) are considered here. Given the parameters chosen for the model, the branching ratios BR($\rho_T \rightarrow \pi_T^\pm Z^0$) are 39.8%, 38.2% and 13.0% respectively. In all cases, $\pi_T^\pm$ decays to $c\bar{b} \sim 92\%$ of the time (assuming that the $t\bar{b}$ channel is closed or highly suppressed, as in TC2 models). To obtain the overall branching ratio, one must multiply by BR($Z \rightarrow \ell^+\ell^-$)=6.7% ($\ell = e$ or $\mu$).

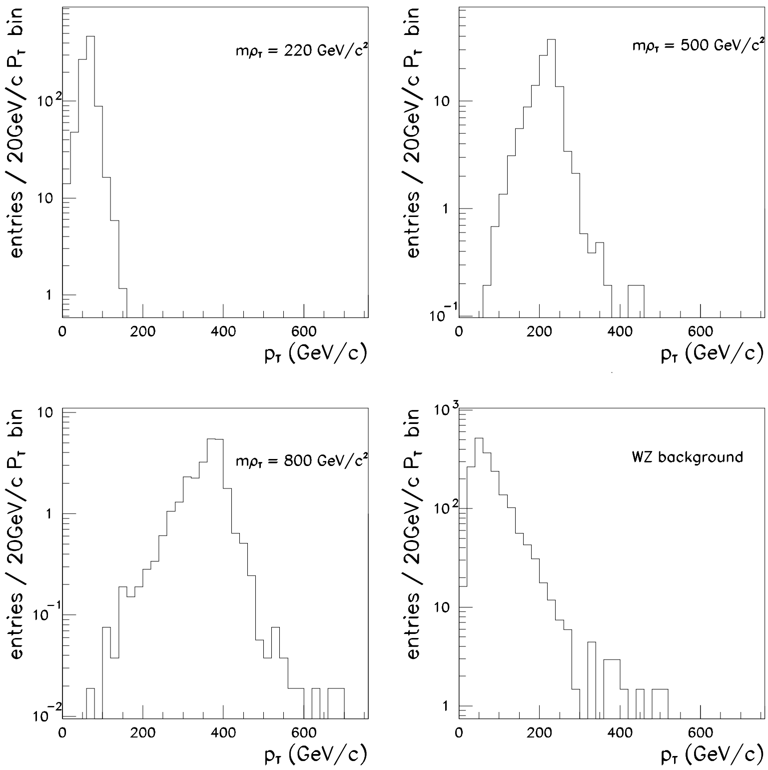


Figure 3: $\rho_T^\pm \to W^\pm Z^0 \to \ell^\pm \nu \ell^+ \ell^-$: Transverse momentum of the reconstructed Z from different $\rho_T^\pm$ masses and from the WZ background.

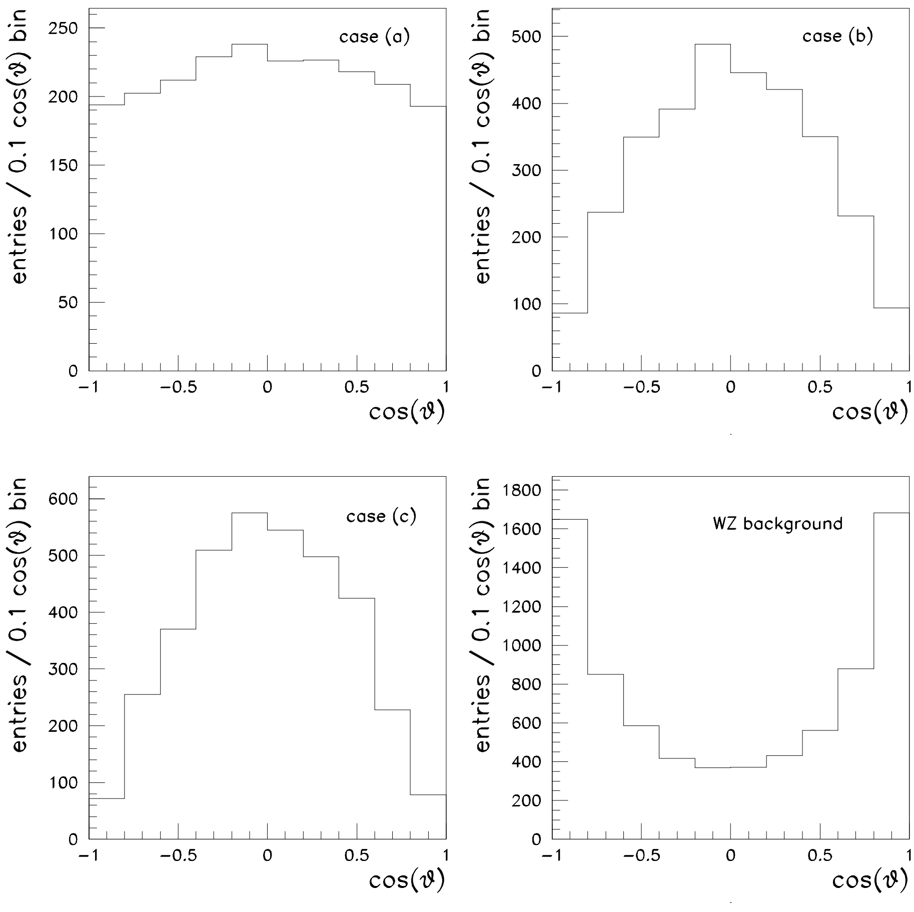


Figure 4: $\rho_T^\pm \to W^\pm Z^0 \to \ell^\pm \nu \ell^+ \ell^-$: Distribution of decay angles of the $\rho_T$ candidates for three cases of $\rho_T$ production and for $WZ$ background.

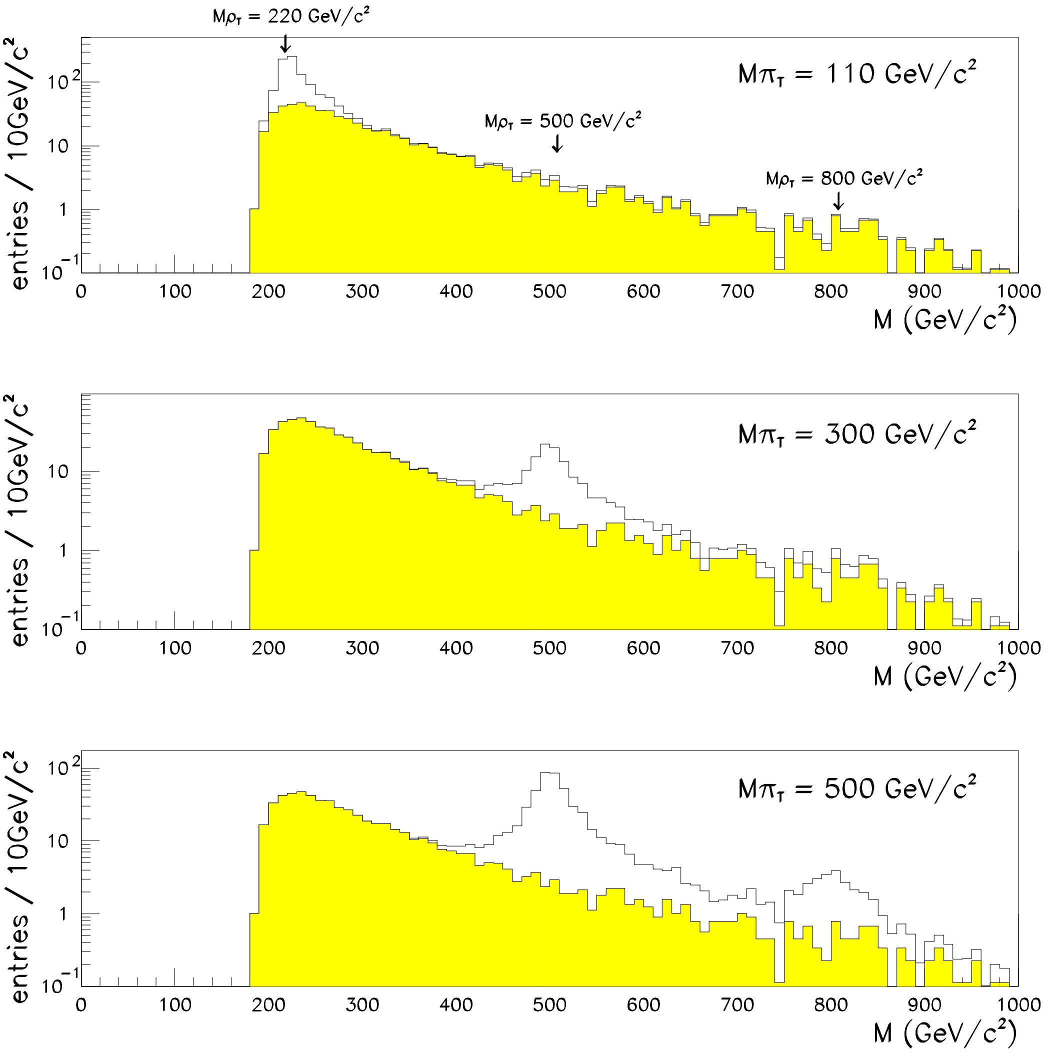


Figure 5: $\rho_T^{\pm} \rightarrow W^{\pm}Z^0 \rightarrow \ell^{\pm}\nu\ell^{+}\ell^{-}$: Reconstructed W$^{\pm}$Z$^{o}$ invariant mass. The solid line is for the $\rho_T$ signal and the filled area for the WZ background. The three diagrams show the different $\rho_T$ for the cases where $m_{\pi_T}$ = 100, 300 and 500 GeV/c$^2$.

| case | (a) | (e) | (b) | (f) | (g) | (h) | (c) |
|---|---|---|---|---|---|---|---|
| signal events | 484 | 4 | 89 | 376 | 0.7 | 237 | 20 |
| background | 134 | 24 | 24 | 24 | 6 | 6 | 6 |
| $S/\sqrt{B}$ | 31.6 | 0.7 | 14.7 | 64.2 | 0.3 | 1.2 | 10.9 |
| $\sigma \times BR$ | | | | | | | |
| model | 0.16 | $1.04\ 10^{-3}$ | $1.3\ 10^{-2}$ | $5.4\ 10^{-2}$ | $1.5\ 10^{-4}$ | $3.6\ 10^{-4}$ | $2.5\ 10^{-3}$ |
| for $5\sigma$ significance | 0.025 | $7.43\ 10^{-3}$ | $0.44\ 10^{-2}$ | $0.42\ 10^{-2}$ | $2.5\ 10^{-3}$ | $1.5\ 10^{-3}$ | $1.2\ 10^{-3}$ |

Table 3: Expected significance for the signal $\rho_T^\pm \to W^\pm Z^0 \to \ell^\pm \nu \ell^+ \ell^-$ after event selection.

The principal backgrounds are: Z + jets (consisting of $qq \to gZ$, $qg \to qZ$ and $qq \to ZZ$), $t\bar{t}$, and continuum WZ production ($q\bar{q} \to WZ$, with a preselection requiring $p_T > 30$ GeV). Table 4 shows the cross sections of signals and backgrounds, and the number of events used for the simulation.

| Process | preselection | $\sigma$ (pb) | Nb. of events simulated |
|---|---|---|---|
| $\rho_T$ case (b) | $\hat{m} > 100$ GeV/c$^2$ | 4.29 | $2.2 \times 10^5$ |
| $\rho_T$ case (c) | $\hat{m} > 600$ GeV/c$^2$ | 0.77 | $1.22 \times 10^5$ |
| $\rho_T$ case (d) | $\hat{m} > 600$ GeV/c$^2$ | 0.735 | $1.30 \times 10^5$ |
| Z + jets | $Z \to \ell^+\ell^-$; $\hat{p}_T > 100$ GeV/c | 85.5 | $10^6$ |
| | $80 < \hat{p}_T < 100$ GeV/c | 74.7 | $10^5$ |
| $t\bar{t}$ | $\hat{p}_T > 100$ GeV/c | 333 | $5.3 \times 10^6$ |
| WZ | $\hat{p}_T > 30$ GeV/c | 20.6 | $10^6$ |

Table 4: Signals and backgrounds for the observation of $\rho_T^\pm \to \pi_T^\pm Z^0 \to bq\ell^+\ell^-$

The cuts used in this analysis are the following:

2A. Two same flavor, opposite charge leptons required, with $p_T^{\ell_1} > 60$ GeV/c and $p_T^{\ell_2} > 20$ GeV/c.

2B. The invariant mass of the lepton pair should be close to the mass of the Z: $|m_{\ell\ell} - 91.\text{GeV}| < 5.$ GeV. The histogram of $m_{\ell\ell}$ is shown in fig. 6

2C. One identified b-jet is required. The highest $p_T$ b-jet is assumed to come from the technipion decay. It must satisfy the conditions: $|\eta_b| < 2$ and $p_T^b > 100$ GeV.

2D. At least one jet, not identified as a b-jet is required. The highest energy jet is the candidate. It must satisfy $|\eta_j| < 2$ and $p_T^j > 100$ GeV.

2E. In order to tune the next cut, we exclude the low mass regions and restrict ourselves to events having $m_{bj} > 150$ GeV and $m_{\ell\ell bj} > 300$ GeV. In the rest frame of the $bj\ell\ell$ system (the $\rho_T$), we accept only events for which the angle of decay with respect to the direction of the $\rho_T$ is $|\cos\hat{\theta}_{llbj}| < 0.6$ This cut is justified in fig. 7. This angle is sensitive to the polarization of the $\rho_T$.

2F. We further require $|\eta_b - \eta_j| < 2$

Fig. 8 shows the signals and backgrounds expected with the above selection after 3 years of low luminosity running (integrated luminosity of 30 fb$^{-1}$). The statistical fluctuations represent the generated statisitics and are consequently exaggerated. Cases (b) and (c) give clear signals above background, but case (d) is not resolved from background, not only because of its small number of events, but also because of the larger width, 77 GeV, of the $\rho_T$ resonance.

A better resolution of 2-jet systems would considerably improve the signal to background ratio. As is shown in fig. 9, the difference in the reconstructed masses $m_{\rho_T}$ and $m_{\pi_T}$ is better resolved than the individual masses separately, since uncertainties in jet pair mass measurement largely cancel. An improved jet pair resolution can be achieved by choosing a larger cone for jet reconstruction. Fig. 10 shows the effect of selecting a value of $\Delta R = 0.7$ instead of $\Delta R = 0.4$. However, by doing so, we would become more susceptible to pileup from minimum bias events, and other detector effects. In order to extract the significance of the signals (see table 5), we count the number of signal and background events in mass regions around the signal peak in the following way: for cases (b), (c) and (d), the selected regions were $\{m_{\rho_T} - m_{\pi_T}, m_{\pi_T}\}$ = {175-230,200-350}, {250-350,350-600} and {420-620,190-280} respectively (in GeV). It was verified that the results do not change significantly if a cone of size $\Delta R = 0.7$ is used. The systematic error due to the uncertainty in the shape of the background is not included.

# 3 $\rho_T^\pm \to W^\pm \pi_T^0 \to \ell^\pm \nu b\bar{b}$

With the multiscale technicolor model parameters used, the branching ratio BR($\rho_T \to W^\pm {\pi_T}^0$)= 36.3%, 38.2% and 13.2% for cases (b), (c) and (d) respectively. The ${\pi_T}^0$ decays 90% of the time to $b\bar{b}$ (assuming that the $t\bar{t}$ channel is closed, as in the TC2 model). The overall branching ratio must include BR($W^\pm \to \ell^\pm\nu$)=21.6% ($\ell = e$ or $\mu$). It must be noted that, however, that the decay of a coloured technipion to a pair of gluons may have a dominant branching ratio. This case has been analysed for the Tevatron energy [18].

The backgrounds considered here are: $t\bar{t}$, W + jets (consisting of: $qq \to W$, $qq \to gW$, $qq \to WW$ and $qg \to fW$), Z+jets and WZ. Background from $Wb\bar{b}$ production, which should represent a subset of the W+jets background has also been generated with a code

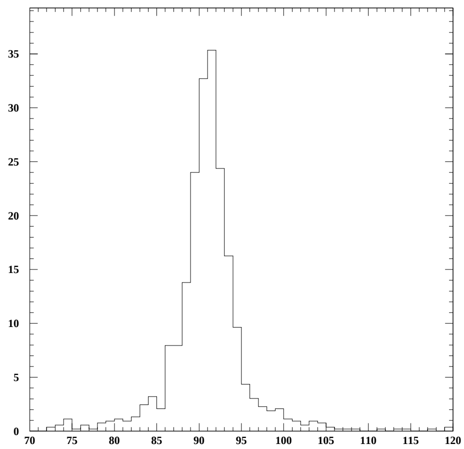

Figure 6: $\rho_T^\pm \to \pi_T^\pm Z^0 \to bq\ell^+\ell^-$: Reconstructed masses of $Z \to \ell\ell$ for $\rho_T$ of case (c).

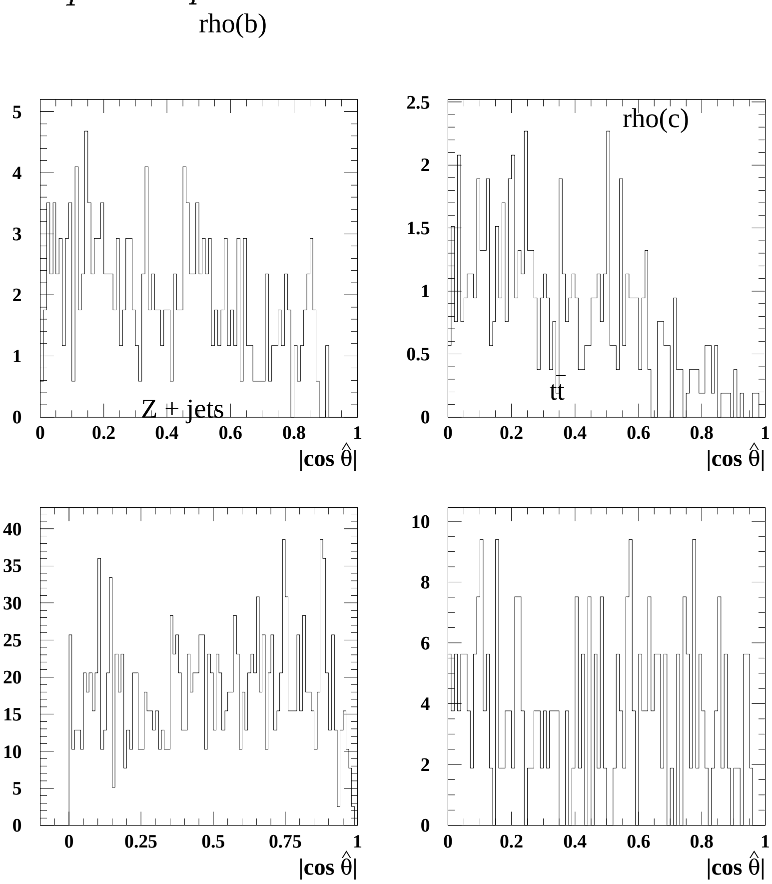


Figure 7: $\rho_T^\pm \to \pi_T^\pm Z^0 \to bq\ell^+\ell^-$: Distribution of $|\cos\hat{\theta}_{llbj}|$ for $\rho_T$(b), $\rho_T$(c), Z+jets, and $t\bar{t}$.

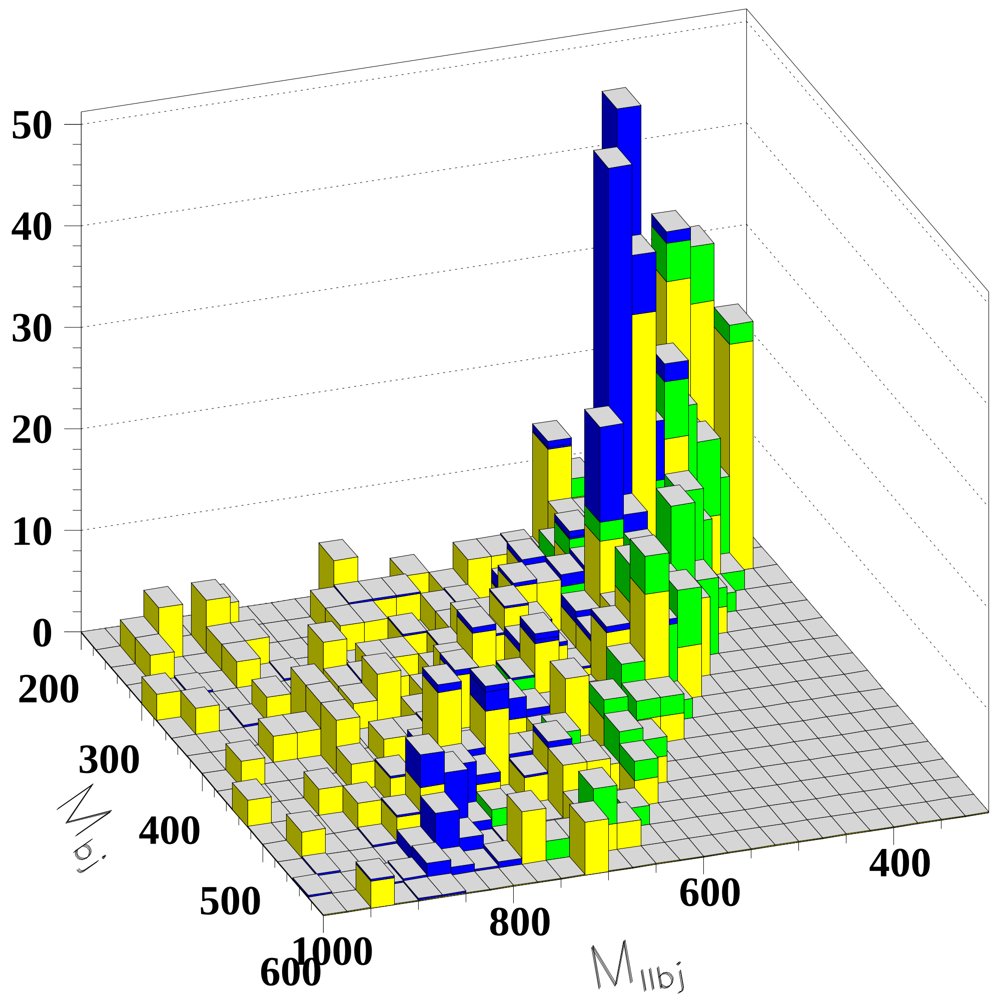


Figure 8: Reconstructed masses of $\rho_T$ candidates and $\pi_T$ candidates in the decay $\rho_T^{\pm} \rightarrow \pi_T^{\pm} Z^0 \rightarrow bq\ell^+\ell^-$. The Z+jets background is in blue, and the ttbar background in green. The three cases (b), (c) and (d) are shown in red.

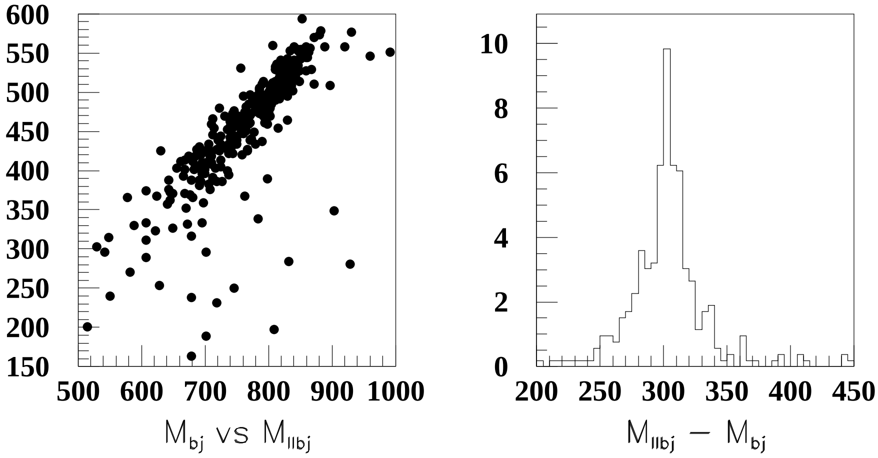


Figure 9: $\rho_T^{\pm} \to \pi_T^{\pm} Z^0 \to bq\ell^+\ell^-$: Distribution of surviving events, after all cuts, for case (c).

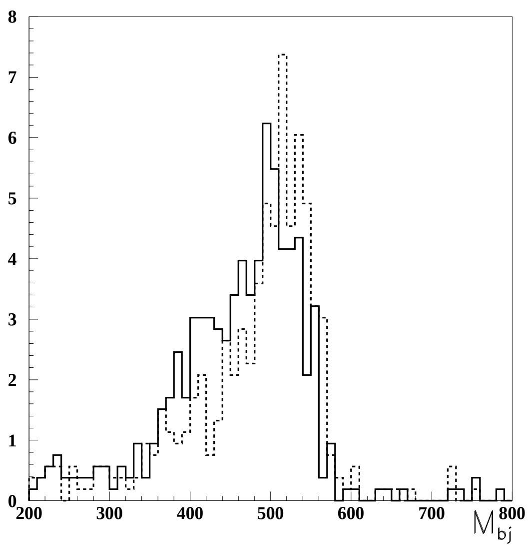


Figure 10: $\rho_T^{\pm} \to \pi_T^{\pm} Z^0 \to bq\ell^+\ell^-$: Comparison of reconstructed $M_{bj}$ for jet cones of size $\Delta R = 0.4$ (full histogram) and $\Delta R = 0.7$ (dashed histogram).

| Cut | $\rho_T$ case (b) | $\rho_T$ case (c) | $\rho_T$ case (d) |
|---|---|---|---|
| 2A-2B | 435/2800/145 | 92/875/41 | 32/1265/26 |
| 2C | 247/ 859/ 62 | 76/389/ 9 | 21/ 427/1.9 |
| 2D | 144/ 169/ 24 | 58/ 77/ 1.9 | 12/ 111/1.9 |
| 2E-2F | 115/ 116/ 17 | 48/ 44/ 1.9 | 11/ 49/0 |
| $S/\sqrt{B}$ | 10.0 | 7.1 | 1.6 |
| $\sigma \times BR$ (pb) | | | |
| model | 0.104 | 0.018 | 0.0059 |
| for $5\sigma$ significance | 0.052 | 0.013 | 0.018 |

Table 5: $\rho_T^\pm \to \pi_T^\pm Z^0 \to bq\ell^+\ell^-$: Number of signal/Z+jets/$t\bar{t}$ events around the mass peak of the signal, after the application of successive cuts (see the text). The last two lines give the $\sigma \times BR$ predicted by the model, with the assumed values of the parameters, as well as the $\sigma \times BR$ required for a $5\sigma$ significance of the signal

obtained from ref [19], running of HERWIG 5.6, for the purpose of checking. The cross sections of signals and backgrounds, as well as the number of events generated for the simulation are shown in table 6.

| Process | preselection | $\sigma$ (pb) | Nb. of events simulated |
|---|---|---|---|
| $\rho_T$ case (b) | $\hat{m} > 100$ GeV/c$^2$ | 4.29 | $2.2 \times 10^5$ |
| $\rho_T$ case (c) | $\hat{m} > 600$ GeV/c$^2$ | 0.77 | $1.22 \times 10^5$ |
| $\rho_T$ case (d) | $\hat{m} > 600$ GeV/c$^2$ | 0.735 | $1.30 \times 10^5$ |
| $t\bar{t}$ | $\hat{p}_T > 100$ GeV/c | 333 | $5.3 \times 10^6$ |
| W + jets | $W \to \ell\nu$; $\hat{p}_T > 100$ GeV/c | 638 | $6 \times 10^6$ |
| $Wb\bar{b}$ | | 19.9 | $2 \times 10^5$ |
| Z + jets | $Z \to \ell^+\ell^-$ $\hat{p}_T > 100$ GeV/c | 85.5 | $6 \times 10^5$ |
| WZ | | 20.6 | $10^6$ |

Table 6: Signals and backgrounds for the observation of $\rho_T^\pm \to W^\pm \pi_T^0 \to \ell^\pm \nu b\bar{b}$

Events are selected according to the following criteria:

3A. One lepton is required, having $p_T > 30$ GeV and $|\eta| < 2$.

3B. Two reconstructed b jets are required. They must be in the central region ($|\eta| < 2$). The most energetic one must have $p_T > 100$ GeV and the other $p_T > 50$ GeV.

3C. The missing transverse energy should be $E_T^{\rm miss} > 50$ GeV.

3D. Efficient reduction of the dominant $t\bar{t}$ background can be achieved by applying a jet veto. No extra jet, with $p_T > 40$ GeV, besides the two b-jets are allowed.

3E. In order to tune the next cut, we restrict ourselves to events having $m_{bb} > 150$ GeV/c$^2$ and $m_{\ell\nu bb} > 300$ GeV/c$^2$.

3F. The $W$ is reconstructed from the lepton and $E_T^{\rm miss}$ four-momenta (the longitudinal momentum of the neutrino is calculated to give the correct $W$ mass, up to a two-fold ambiguity). We require that the two corresponding solutions for the reconstructed mass of the $\rho_T$ not differ significantly: $|m^{(1)}_{\ell\nu bb} - m^{(2)}_{\ell\nu bb}| < 80$ GeV/c$^2$. This cut is found to be efficient at rejecting events which do not contain a $W$ and for which the two solutions are very different.

3G. For each of these solutions, we consider the following cut: in the rest frame of the $l\nu bb$ system, we require that the decay angle with respect to the direction of the $\rho_T$ be $|\cos\hat{\theta}_{bb}| < 0.6$. The importance of this cut is seen in fig. 11.

Fig. 12 shows the signals and backgrounds expected with the above selection with 30 fb$^{-1}$. Both solutions are included in the histogram, with weight 0.5 each. Clear signals can be seen above background for some of the above cases, although poor $m_{bb}$ resolution is obtained. The significance of the signals that would be obtained is given in table 7. The following windows were used for the peak regions: $\{m_{bb}, m_{l\nu bb} - m_{bb}\} = \{$230-340,170-270$\}$, $\{$300-560,200-400$\}$, $\{$180-300,380-620$\}$ GeV, for cases (b), (c) and (d) respectively. Also shown in table 7 are the $\sigma \times BR$ required for a $5\sigma$ significance. One notes that the $Wb\bar{b}$ background is generally a small fraction of the W + jets background. The two bjets from the former sample of events are usually softer than the jets from the latter, and are therefore less important in the signal regions. The uncertainty in the shape of the background can constitute an important systematic error.

# 4 $b\bar{b}$ resonances

Color-octet technipions have a higher production cross section through $gg$ fusion than color-singlet due to color counting factors. Since they couple to ordinary fermions proportionally to the square of their mass, they will decay to the highest mass pair possible, the signal would be a $b\bar{b}$ or $t\bar{t}$ resonance. It must be noted that the decay to $gg$ pairs compete with these channels and may dominate. Other $b\bar{b}$ resonances are predicted by topcolor models, where the topgluon splits into heavy quarks. The mass reach of such topgluons at the Tevatron (2 fb$^{-1}$) has been estimated to be close to 1 TeV, depending on the width [20] Since the models of production and decay vary enormously, the analysis will be viewed here as a generic search for single production of techniparticle. For the purpose of this study, the process of $\eta_8$ production by gluon-gluon fusion, as implemented

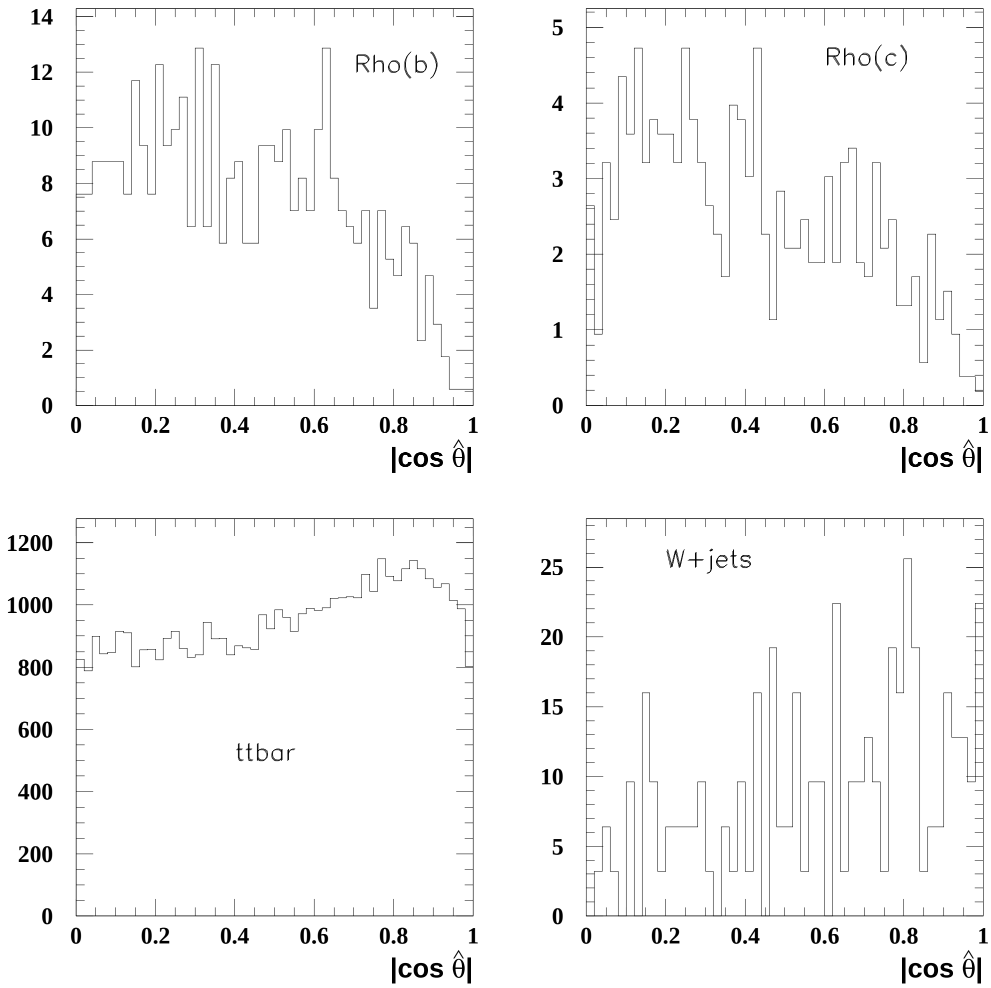


Figure 11: Distribution of $\cos\hat{\theta}_{lvbb}$ for $\rho_T$ of cases (b) and (c) as well for the $t\bar{t}$ and W+jets backgrounds. Cuts 3A-3E (excluding 3D) have been applied.

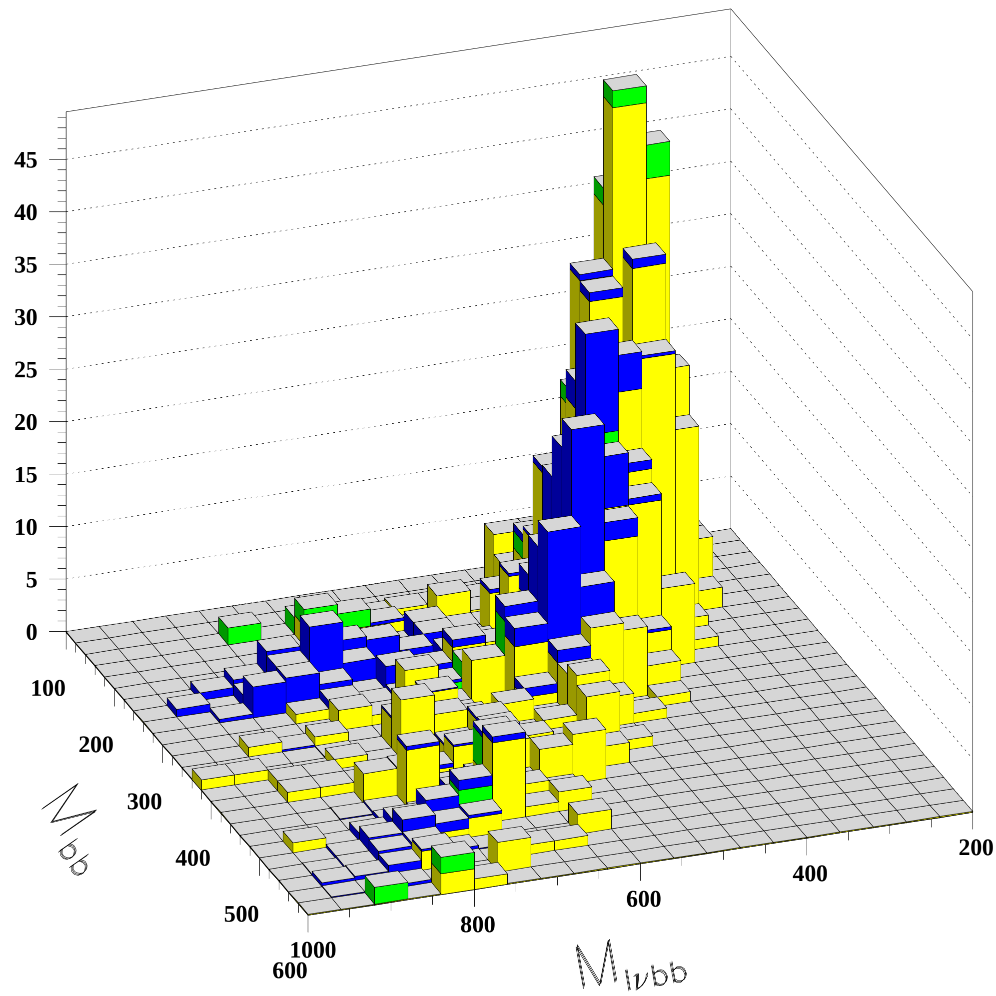


Figure 12: Reconstructed masses of $\rho_T$ candidates vs $\pi_T$candidates in the channel $\rho_T^{\pm} \to W^{\pm}{\pi_T}^0 \to \ell^{\pm}\nu bb$. The W+jets background is in blue, and the ttbar background in green. Other backgrounds are negligible. The three cases (b), (c) and (d) are shown in red.

| Cut | $\rho_T$ case (b) | $\rho_T$ case (c) | $\rho_T$ case (d) |
|---|---|---|---|
| 3A-3B | 417/11400/6/77 | 122/9114/3/112 | 45/2300/16/82 |
| 3C | 235/6900/4/38 | 93/6300/3/69 | 38/1980/7/65 |
| 3D | 122/357/3/7 | 33/285/3/24 | 17/74/4/12 |
| 3E-3F | 106/251/3/5 | 26/160/3/15 | 13/7/3/0 |
| 3G | 86/165/1/5 | 24/118/3/10 | 12/5/3/0 |
| $S/\sqrt{B}$ | 6.6 | 2.1 | 4.2 |
| $\sigma \times BR$ (pb) | | | |
| model | 0.336 | 0.064 | 0.021 |
| for $5\sigma$ significance | 0.255 | 0.15 | 0.025 |

Table 7: $\rho_T^{\pm} \to W^{\pm}\pi_T^0 \to \ell^{\pm}\nu b\bar{b}$: Number of signal/$t\bar{t}$/$Wb\bar{b}$/(W+jets and Z+jets) events around the mass peak of the signal, after the application of successive cuts (see the text) for an integrated luminosity of 30 fb$^{-1}$. The last two lines give the $\sigma \times BR$ predicted by the model, with the assumed values of the parameters, as well as the $\sigma \times BR$ required for a $5\sigma$ significance of the signal

in PYTHIA according to the one-family model [21, 22] is used here. The $\eta_8$ is a color octet technimeson. The mass has been chosen to be 300 GeV, *i.e.* below the $t\bar{t}$ threshold. Generic vector resonances, such as topgluons, of masses 500, 1000 and 2000 GeV have also been studied.

The backgrounds considered for this process are: hard QCD (with $\hat{p}_T > 80$ GeV/c and $\sqrt{\hat{s}} > 200$ GeV) and $t\bar{t}$.

To extract the signal, the only selection was to require at least two identified b-jets with a minimum value of $p_T$ in the region $|\eta| < 2$. Since a b trigger is not implemented in ATLAS, the LVL1 trigger J75 x3 (i.e. 3 jets with $p_T > 75$ GeV) will be required in the search for the 300 GeV resonance. For the other higher resonances considered, the single jet trigger J180 will suffice. Events having a third jet are rejected if $p_T > p_{T3}(\max)$ (see table 8). Table 8 also shows the required $\sigma \times BR$ required for a $5\sigma$ discovery. In each case, the resonance would be seen as a small, but statistically significant peak on top of a very large, steeply falling background. In this study, the assumed intrinsic widths of the resonances were very narrow. For wider resonances, the intrinsic width must be added in quadrature with $\sigma_m$, shown in table 8 and a new estimate of $\sigma \times BR$ obtained.

# 5 $t\bar{t}$ resonances

This is the same case as above, but with a technipion sufficiently massive, 500 GeV/c$^2$, to decay to $t\bar{t}$ pairs. Although the decay of a technipion to $t\bar{t}$ is highly suppressed in

| $m_{bb}$ | $p_T^{min}$ $(b_1/b_2)$ | $p_{T3}^{max}$ | $\sigma_m$ (GeV) | $\sigma \times BR$ $(5\sigma)$ (pb) |
|---|---|---|---|---|
| 300 | 75/75 | 100 | 37 | 13 |
| 500 | 180/50 | 50 | 60 | 7.0 |
| 1000 | 200/100 | 100 | 70 | 0.57 |
| 2000 | 300/200 | 100 | 160 | 0.11 |

Table 8: $b\bar{b}$ resonance: dicovery limits, with 30 $\text{fb}^{-1}$, for narrow $b\bar{b}$ resonances of different masses, after cuts on the minimaum $p_T$ of the reconstructed b jets, and a maximum $p_T$ of any third jet. Also shown is the approximate width of the reconstructed resonance.

topcolor assisted technicolor models, other resonances, such as a topgluon are predicted by such models. Salar fields decaying to $t\bar{t}$ are also predicted as scalar bound states of two mirror fermions in other models of alternative symmetry breaking [23]. As for the $b\bar{b}$ study above, the process of $\eta_8$ production, implemented in PYTHIA is used here.

The backgrounds are:

(i) W+jets (with $\hat{p}_T > 80$ GeV). Only events having at least one lepton and one b-jet (before b-tagging) have been generated for this analysis.

(ii) $t\bar{t}$, with a requirement of $\hat{p}_T > 80$ GeV. Only events with one lepton have been generated.

(iii) hard QCD (with $\hat{p}_T > 80$ GeV/c and $\sqrt{\hat{s}} > 200$ GeV). The cuts applied at generator level do not affect significantly the results below.

The mass of the $\eta_8$ is reconstructed by looking for the channel $t\bar{t} \to \ell\nu b\ bjj$. The following selection criteria are applied:

6A. One lepton having $p_T > 20$ GeV and within $|\eta| < 2$ is required for the trigger.

6B. Two b jets are required, with $p_T > 60$ GeV/c and 40 GeV, and within $|\eta| < 2$. Two additional jets, not identified as b-jets are required, with $p_T > 50$ GeV and 40 GeV, also within $|\eta| < 2$.

6C. $E_T^{\text{miss}}$ must be $> 20$ GeV.

6D. At that point, the W from the $t \to Wb \to \ell\nu b$ decay is reconstructed, using $E_T^{\text{miss}}$ and the lepton momentum. There is a two-fold ambiguity in the solution. There is also a two-fold ambiguity in assigning the two highest $p_T$ b-jets to the two highest energy light-quark jets. These ambiguities are resolved by choosing the solution that gives top masses closest to the true mass of the top (175 GeV). The 4th cut is then $160 < m_t^\ell < 195$ GeV and $160 < m_t^h < 220$ GeV, where $m_t^\ell$ and $m_t^h$ are the reconstructed masses of the top quarks for which the W decays leptonically and hadronically, respectively.

This simple procedure gives top-mass resolution as shown in fig. 13. The $t\bar{t}$ resonance mass is then reconstructed with a resolution of about 57 GeV. Table 9 shows the discovery limits for resonances of masses 500, 750 and 1000 GeV for an integrated luminosity of 10 fb$^{-1}$ and for 100 fb$^{-1}$.

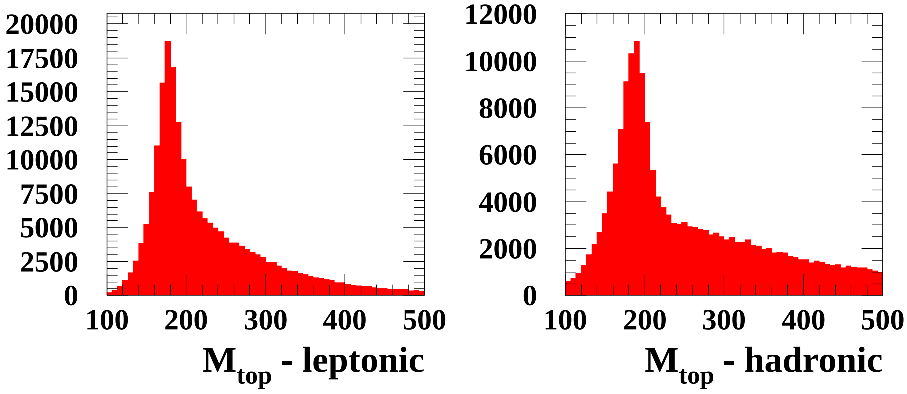


Figure 13: $\eta_8 \rightarrow t\bar{t}$: Reconstructed masses of top in $t\bar{t}$ decays. The left histogram shows the mass of the top for which the W decays leptonically and the one on the right shows the mass of the other top, for which the W decays hadronically

| $m_{t\bar{t}}$ (GeV) | $\Gamma(t\bar{t})$ (GeV) | $\sigma \times BR$ | |
|---|---|---|---|
| | | 10 fb$^{-1}$ | 100 fb$^{-1}$ |
| 500 | 57 | 17 | 5.5 |
| 750 | 107 | 7.3 | 2.30 |
| 1000 | 152 | 2.55 | 0.81 |

Table 9: $t\bar{t}$ resonance: masses and natural widths assumed for the study of technicolor resonances. Also shown are the minimum values of $\sigma \times BR$ necessary for a $5\sigma$ discovery significance for integrated luminosities of 10 fb$^{-1}$ and 100 fb$^{-1}$.

# 6 $\omega_T \to \gamma\pi_T^0 \to \gamma b\bar{b}$

The $\omega_T^0$ particle is a vector particle of isospin 0. One of its clean decay modes is $\omega_T \to \gamma\pi_T^0$. A search for this resonance has been performed at CDF [24]. Here, we have investigated two cases:
(i) $m_{\omega_T}$ = 500 GeV/c$^2$, with width 0.32 GeV and $m_{\pi_T^0}$=300 GeV/c$^2$. The cross section for production is 0.51 pb, according to the model used here [13, 14], as implemented in PYTHIA, and the branching ratio to $\gamma\pi_T^0$ is 87%.
(ii) $m_{\omega_T}$ = 800 GeV/c$^2$, with width 1.0 GeV and $m_{\pi_T^0}$=300 GeV/c$^2$. The cross section for production is 0.093 pb, and the branching ratio to $\gamma\pi_T^0$ is 94%. These assumed branching ratios do not account for decay branches to transversely polarized gauge bosons [15].

For the simulation of the background, a Monte Carlo program for generation of $\gamma b\bar{b}$, provided by M. Mangano [25] was used. We have considered backgrounds from $qq \to g\gamma$, $qg \to q\gamma$ and $gg \to g\gamma$ (processes 14, 29 and 115 of PYTHIA), as well as general QCD background with initial and final state radiation. Backgrounds from misidentified photon jets, which are not taken into account, are small, given the rejection that ATLAS obtains, for example in the study of the $H \to \gamma\gamma$ process.

To extract the signal, we require

7A. the presence of one photon with $p_T^\gamma > 50$ GeV/c within $|\eta < 2|$

7B. the presence of 2 identified b-jets, each having $p_T > 40$ GeV/c, and falling within $|\eta < 2|$

7C. the difference in azimuthal angles between the two b-jets to be > 2 radians, as we expect them to be mostly back to back for a heavy decaying system.

With these selection criteria, the signals that remain are shown in fig. 14. The results do not account for a possible inefficiency in photon reconstruction (possibly a 20There is a very significant signal for the lower-mass $\omega_T$. The higher mass case is less prominent but still significant. Table 10 gives the observed significances and $\sigma\times$ BR required for a 5 $\sigma$ significance with 30 fb$^{-1}$, for both the lower and higher mass $\omega_T$, in the mass windows $[250 < m_{bb} < 350;\ 180 < m_{\gamma bb} < 220]$ and $[400 < m_{bb} < 600;\ 280 < m_{\gamma bb} < 330]$ respectively.

# 7 Conclusion

We have examined the observability of technicolor signals in ATLAS, in selected regions of mass for the techniparticles. Good jet-pair resolution is essential for such studies. In

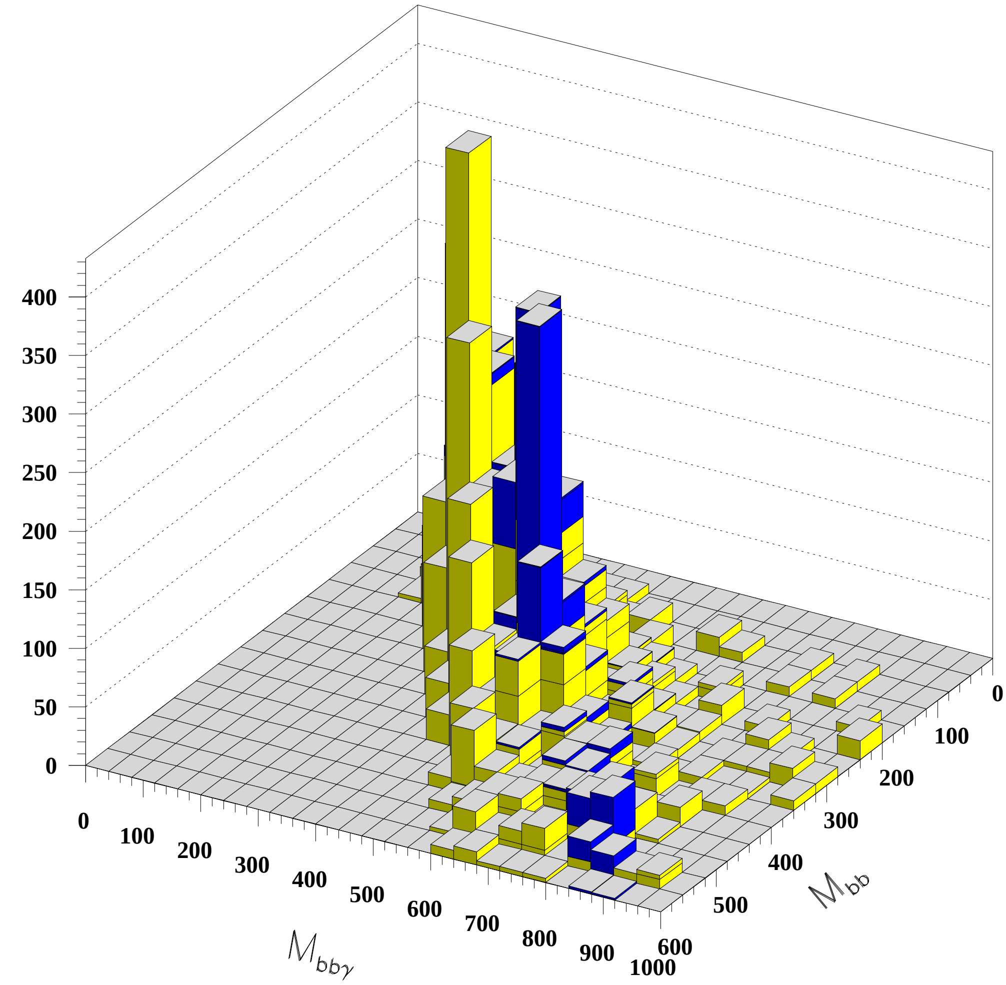


Figure 14: $\omega_T \to \gamma\pi_T^0 \to \gamma b\bar{b}$: Reconstructed masses of bb-jet system versus the mass of the $\gamma bb$ system. Two scenarios are considered for the signal: $\omega_T$ of mass 800 GeV/c$^2$ and 500 GeV/c$^2$ decaying to $\pi_T$ of mass 500 GeV/c$^2$ and 300 GeV/c$^2$ respectively. The signals are in red. In blue is the prompt photon background. QCD leaves no entry in this histogram (but with a multiplicative factor of 17700).

| | $\omega_T(500)$ | $\omega_T(800)$ |
|---|---|---|
| Nb of events | 612/105 | 174/24 |
| S/$\sqrt{B}$, model | 60 | 35 |
| $\sigma\times$ BR, model | 0.161 | 0.033 |
| $\sigma\times$ BR required for 5 $\sigma$ | 0.013 | 0.0046 |

Table 10: $\omega_T \to \gamma\pi_T^0 \to \gamma b\bar{b}$: Number of signal/$\gamma$+jets events around the mass peak of the signal. The $\sigma \times BR$ predicted by the model, with the assumed values of the parameters, as well as the $\sigma \times BR$ required for a $5\sigma$ significance of the signal are also shown.

all cases, we have estimated lower limits required for a 5-$\sigma$ significance with 30 fb$^{-1}$. The dominant production process is $q\bar{q}$ production, but the vector boson fusion process is also important since it provides the signature of forward jet tagging. Although in some cases signals are below the clear observability criterion of $5\sigma$ above background, the combination of signals could provide strong evidence for the existence of techniparticles.

# 8 Acknowlegments

The authors would like to thank K. Lane for useful discussions, and M. Mangano for providing the Monte Carlo for $\gamma$ jet jet production.

# References

[1] T. Hambye and K. Riesselmann, *Phys. Rev.* **D55** (1997) 7255, hep-ph/9708416;
M. Quiros, Publ. in: Perspectives on Higgs physics, 2nd ed. G L Kane World Sci., Singapore, 1997 Advanced Series on Directions in High-Energy Physics ; 17 (148-180), hep-ph/9703412;
A. Ghinculov and T. Binoth, Workshop on Theory of LHC Processes CERN, Geneva, Switzerland ; 9 - 13 Feb 1998 . Publ. in: Proceedings, hep-ph/9807227

[2] R. S. Chivukula, *NATO Advanced Study Institute on Quantum Field Theory Since 1970: Perspective and Prospectives*, Les Houches, 1998 (hep-ph/9803219)

[3] S. Weinberg, *Phys. Rev.* **D19** (1979) 1277;
L. Susskind, *Phys. Rev.* **D20** (1979) 2619

[4] M. Golden and L. Randall, *Nucl. Phys.* **B361** (1991), 3;
R.S. Chivukula *et al.*, hep-ph/9305232 or *Phys.Lett.* **B311** (1993) 157

[5] S. Dimopoulos and L. Susskind, *Nucl. Phys.* **B155** (1979), 237; E. Eichten and K. Lane, *Phys. Lett.* **B90** (1980) 125.

[6] B. A. Dobrescu and J. Terning, BUHEP-97-27 (hep-ph/9709297)

[7] K. Lane, BUHEP-94-24, 27th International Conference on High Energy Physics (ICHEP), Glasgow, Scotland, 1994. (hep-ph/9409304)

[8] M. Knecht and E. de Rafael, Phys.Lett. B424 (1998) 335-342, (hep-ph/9712457)

[9] R. Casalbuoni *et al.*, Nucl. Phys., B : 555 (1999) 3 1/2, hep-ph/9809523;
T. L. Barklow *et al.*, hep-ph/9704217 (Working group summary report from the 1996 DPF/DPB Summer Study, *New Directions in High Energy Physics*, Snowmass, Colorado);
K. Cheung and R.M. Harris, hep-ph/9610382, Summary of New Interactions subgroup of New Phenomena group at Snowass. To appear in the proceedings of DPF/DPB Summer Study on *New Directions for High Energy Physics*, Snowmass, Colorado, 1996;
R. Chivukula *et al.*, hep-h/9503202 (published in *Electroweak Symmetry Breaking and New Physics at the TeV Scale*, World Scientific, T. Barklow, ed., 1996);
E. Eichten *et al.*, Rev. Mod. Phys. 56 (1984) 579, Rev. Mod. Phys. 58 (1986) 1065

[10] E. Eichten, K. Lane and J. Womersley, hep-ph/9704455 or Phys.Lett. B405 (1997) 305-311

[11] T. Sjöstrand, *PYTHIA 5.7 and JETSET 7.4*, Comp. Phys. Commun. 82 (1994) 74 (Version 6.1 obtained from http://www.thep.lu.se/tf2/staff/torbjorn/Pythia.html)

[12] E. Richter-Was et al., *ATLFAST, a package for particle-level analysis.* ATLAS internal note

[13] K. Lane, hep-ph/9605257;
28th International Conference on High-Energy Physics : ICHEP '96 Warsaw, Poland ; 25 - 31 Jul 1996 . Publ. in: Proceedings Z Ajduk and A K Wróblewski, World Sci., Singapore, 1997 (367-377) (or hep-ph/9610463)

[14] E. Eichten and K. Lane, *Phys. Lett.* **B388** (1996) 803 (hep-ph/9607213)

[15] K. Lane, hep-ph/9903369 and hep-ph/9903372

[16] G. Azuelos, R. Mazini and S.R. Slabospitsky, *$\rho_T$ production via $W_L Z_L$ fusion at Hadronic colliders*, ATLAS PHYSICS note, ATL-COM-PHYS-99-067

[17] A. Miagkov, *Vector boson scattering in Chiral Lagrangian model*, ATLAS note ATL-PHYS-99-006

[18] S. Mrenna and J. Womersley, *Phs. Lett.* **B451** (1999) 155.

[19] We thank M. Mangano for providing the code for generation of $Wb\bar{b}$ events.

[20] R. M. Harris, *Discovery Mass Reach for Topgluons Decaying to b anti-b at the Tevatron*, DPF/DPB Summer Study on New Directions for High Energy Physics, Snowmass, Colorado, June 25-July 12, 1996 (hep-ph/9609316)

[21] E. Eichten, I. Hinchliffe, K. Lane and C. Quigg, *Rev. Mod. Phys.* **56** (1984) 579; Rev. Mod. Phys. **58** (1985) 1065

[22] T. Appelquist and G. Triantaphyllou, *Phys. Rev. Lett.* **69** (1992) 2750

[23] G. Triantaphyllou, *Strategies towards Mirror fermion signatures*, hep/ph/9906283

[24] F. Abe et *al.*, CDF Collaboration, *Search for a Technicolor $\omega_T$ Particle in Events with a Photon and a b-quark Jet at CDF*, hep-ex/9810031 or FERMILAB-PUB-98/321-E

[25] We thank M. Mangano for providing the code for generation of $Wb\bar{b}$ events.